JOURNAL OF MATERIALS SCIENCE 37 (2002) 683–687

Synthesis and microstructure of calcia doped ceria as UV filters

M. YAMASHITA, K. KAMEYAMA, S. YABE*
KOSÉ Corporation, 1-18-4 Azusawa, Itabashi-ku, Tokyo 174-0051 Japan
E-mail: sh-yabe@kose.co.jp

S. YOSHIDA
Nippon Inorganic Colour & Chemical CO. LTD., 3-14-1 Funato, Itabashi-ku, Tokyo 174-0041 Japan

Y. FUJISHIRO, T. KAWAI, T. SATO
Institute of Multidisciplinary Research for Advanced Materials, Tohoku University, 2-1-1 Katahira, Aoba-ku, Sendai, Miyagi 980-8577 Japan

Fine particles of calcium oxide doped cerium dioxide, 2–4 nm in diameter, were prepared by the chemical reaction of $CeCl_3$-$CaCl_2$ mixed aqueous solution and NaOH aqueous solution at pH 6–12 and 40°C followed by the oxidation with hydrogen peroxide. Doping of CaO with CeO_2 resulted in decreasing the particle size and consequently, increasing UV shielding efficiency and transparency to visible light. The particle shape of ceria changed significantly depending on the reaction condition, i.e., rod-like particles and spherical particles were formed by the H_2O_2 oxidation of cerium trihydroxide pH above 8 and below 7, respectively.

1. Introduction

Ultrafine titanium dioxide and zinc oxide which are n-type semiconductor possessing ca. 3 eV of band gap energy are effective inorganic sunscreens used in cosmetics, however, their high refractive indices can make the skin look unnaturally white when incorporated into the products. Additionally, their high photocatalytic activity facilitates the generation of reactive oxygen species, which can oxidize and degrade other ingredients in the formulation, raising safety concerns. Cerium dioxide (CeO_2) possessing ca. 3 eV of band gap energy has characteristics ideal in a broad-spectrum inorganic sunscreen: it is quite transparent to visible light, but has excellent ultraviolet radiation absorption properties, and appears natural on the skin without imparting an excessively pale white look. Many workers have prepared cerium dioxide using various methods in order to control the size and morphology of the particles [1–11]. Synthesis of inorganic materials via so-called soft solution chemistry route is a promising method to control the morphology of the products. In a previous paper [12], we succeeded in synthesizing nanoparticles of CeO_2 by the chemical reaction of $CeCl_3$ and NaOH aqueous solutions at 40–60°C. However, nanoparticles of CeO_2 had high catalytic activity for the oxidation of organic materials. The oxidation catalytic activity of CeO_2 could successfully be decreased by coating with amorphous silica [12], but coating with amorphous silica resulted in decreasing UV-shielding effect. It was also found that the oxidation catalytic activity of ceria could be decreased substantially by doping with Ca^{2+} [13]. The morphology and UV-shielding property of nanoparticles of CeO_2 changed significantly depending on the reaction conditions such as pH, etc., however, the details have not been clarified yet. In the present paper a series of test were conducted to evaluate the effect of reaction conditions on the morphology of CaO-doped CeO_2 particles.

2. Experimental method

All chemicals were of reagent grade and used without further purification. The fine powders of calcia doped ceria were prepared by so-called soft solution chemical reactions at 40°C via 3 different routes (Method A-C). At first 100 cm^3 of $CeCl_3$ and $CaCl_2$ mixed aqueous solution ($CeCl_3 + CaCl_2 = 1M$) and stoichiometric amount of 3 M NaOH aqueous solution were simultaneously added to 150 cm^3 of distilled water at 40°C at a flow rate of 0.83 cm^3/min with stirring to precipate Ca^{2+} doped $Ce(OH)_3$. After adjusting the solution to pH 11 with 1M HCl and/or NaOH, 25 cm^3 of 6 wt% H_2O_2 aqueous solution was added at a flow rate of 1.25 cm^3/min to oxidize Ca^{2+} doped $Ce(OH)_3$ to form CaO doped CeO_2. Finally the samples were washed with water and methyl alcohol several times and sufficiently dried at 120°C. These process was designated as Method A. Method B was the same with method A except for adjusting solution pH to 7 before adding H_2O_2 aqueous solution. In Method C, the solutions of NaOH,

*Author to whom all correspondence should be addressed.

$CeCl_3$-$CaCl_2$ and H_2O_2 were simultaneously dropped into 150 cm^3 of distilled water (40°C) with stirring and adjusting pH at 7.

The crystalline phase was determined by X-ray diffraction analysis (Shimadzu XD-01) The morphology of the samples was observed by transmission electron microscopy (TEM)(JEM-1200EX II and JEM-3010 operated at 100 and 300 kV, respectively). The specific surface area of the powders was measured by BET. The UV-shielding properties of the particles were evaluated by measuring the transmittance of the film uniformly dispersed the sample powder with a UV-Vis spectrophotometer (Shimadzu UV-2500PC), where 2 g of powder, 4 g of nitrocellulose of industrial grade, 10 g of ethyl acetate and 9 g of butyl acetate were mixed uniformly using a paint shaker (Asada) and 100 g of 2.7ϕ zirconia ball for 40 h. The dispersion mixture was applied onto a quartz glass plate with an applicator. Thickness of the film was 3 μm after drying at room temperature for 24 h.

3. Results and discussion

3.1. Solubility limit of CaO doped ceria

The composition of precipitate determined by a inductively coupled plasma spectrometry (ICP) are listed in Table I. In the case of the higher final solution pH (Method A), most of ICP data were in fair agreement with the amount of added materials. The results showed that total amount of CaO were doped in CeO_2. But in the case of adding 30 mol% CaO, the precipitate didn't contain 30%mol CaO. It suggested that solubility limit of CaO in CeO_2 is less than 30 mol%. On the other hand, in the case of lower final solution pH (Method B and C), the amount of Ca^{2+} in precipitates were less than those added in the solutions. It might be due to the large solubility of Ca^{2+} below pH 7.

XRD patterns of ceria doped with various amount of calcia formed by Method A are shown in Fig. 1. All peaks could be identified as ceria with fluorite structure of space group *Fm3m* although the peak position slightly shifted to low 2θ angle with increasing CaO content. The samples contained ca. 13 wt% H_2O and showed broad XRD peaks. Therefore, the lattice constants of ceria determined after calcination at 1000°C for 1 hr in order to obtain clear XRD pattern using NaCl as an internal standard are plotted as a function of CaO content in Fig. 2. The lattice constant linearly increased with increasing CaO content up to 20 mol% and then almost constant, indicating the solubility limit is ca. 20 mol% and Ca^{2+} possessing larger ionic size (1.12 Å) simply substitutes for Ce^{4+} (0.97 Å) in CeO_2.

TABLE I The composition of CaO doped CeO_2 with ICP measurement

Ca/(Ca + Ce) added mol%	Analytical value/wt%			Ca/(Ca + Ce) Found mol%
	CeO_2	CaO	H_2O_2	
5	85.40	1.61	13.00	5.48
10	82.80	2.76	14.40	9.30
20	80.30	6.21	13.50	19.20
30	78.90	7.11	14.00	21.70

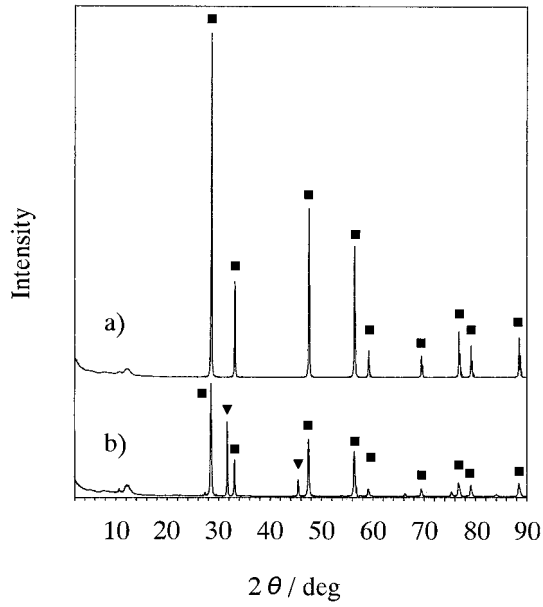

Figure 1 X-ray diffraction profiles of (a) ■ : 20 mol% CaO doped CeO_2 and (b) ■ : undoped ceria, ▼ : NaCl fabricated by Method A.

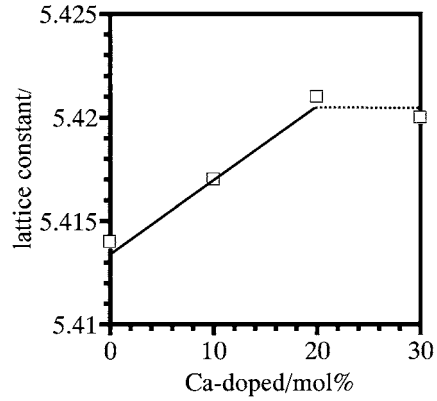

Figure 2 Lattice constant of ceria as a function of CaO content.

3.2. Particle shape and size

TEM images of (a) undoped CeO_2 and (b) 20 mol% CaO doped CeO_2 formed by Method A are shown in Fig. 3, where the solutions were kept above pH 8 during the oxidation reactions of Ce(III) to Ce(IV). Both samples consisted of rod-like particles similar to the cerium hydroxide before H_2O_2 oxidation in both Methods A and B as shown in Fig. 4a but the particle size was significantly different. The particle length of undoped CeO_2 and 20 mol% CaO doped CeO_2 were ca. 40–50 nm and 5–10 nm, respectively, indicating that doping CaO with CeO_2 resulted in decreasing the particle size of ceria. This mechanism has not been fully understood and further study is necessary to clarify it.

On the other hand, the 20 mol% CaO doped CeO_2 particles formed by adjusting the solution pH above 8 and below 7 during the neutralization reaction and oxidation reaction, respectively (method B), were spherical as shown in Fig. 4b. Undoped CeO_2 particles prepared by the similar reaction conditions were also spherical and has similar particle size. It is notable that rod-like and spherical particles of ceria were formed depending on the solution pH during the oxidation reactions of Ce(III) to Ce(IV). In solutions below pH 7

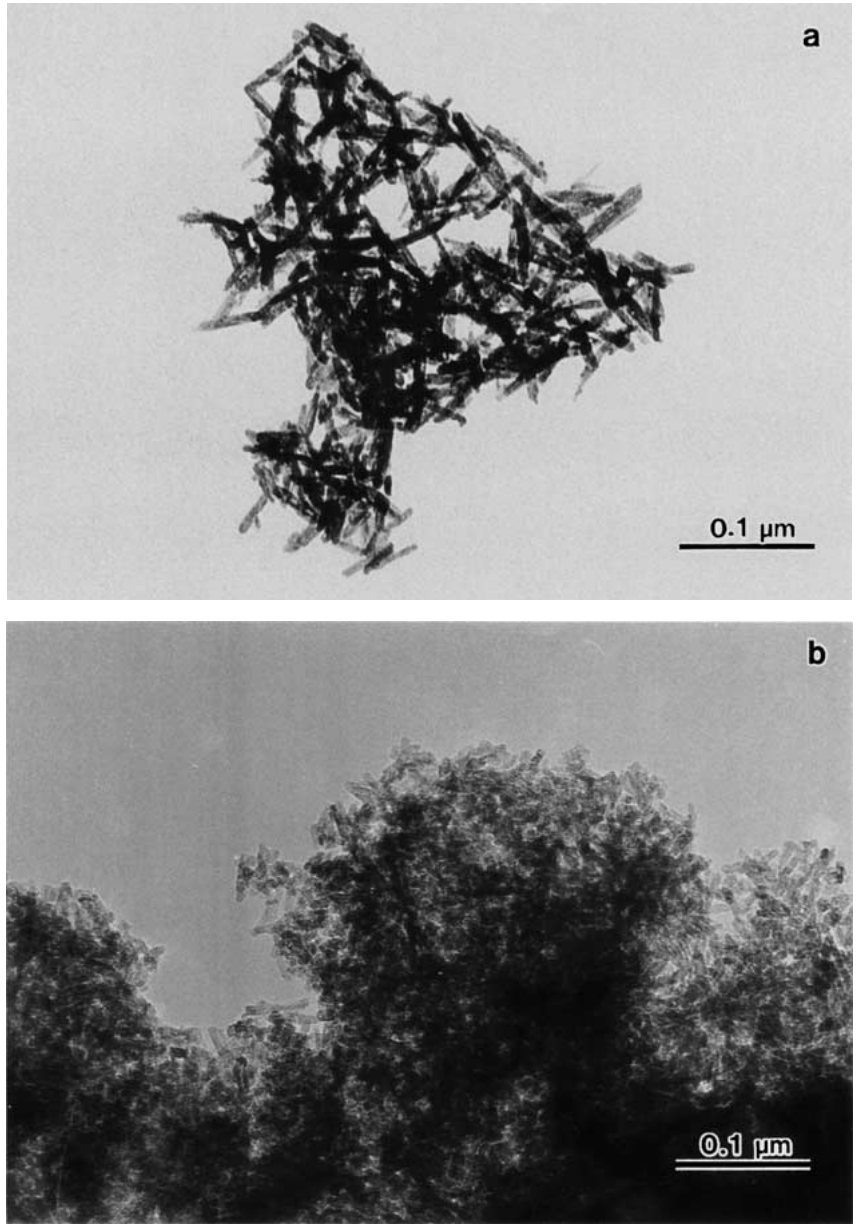

Figure 3 TEM images of (a) undoped CeO_2 and (b) 20 mol% CaO doped CeO_2 formed by Method A (the solution during H_2O_2 oxidation was kept above pH 8).

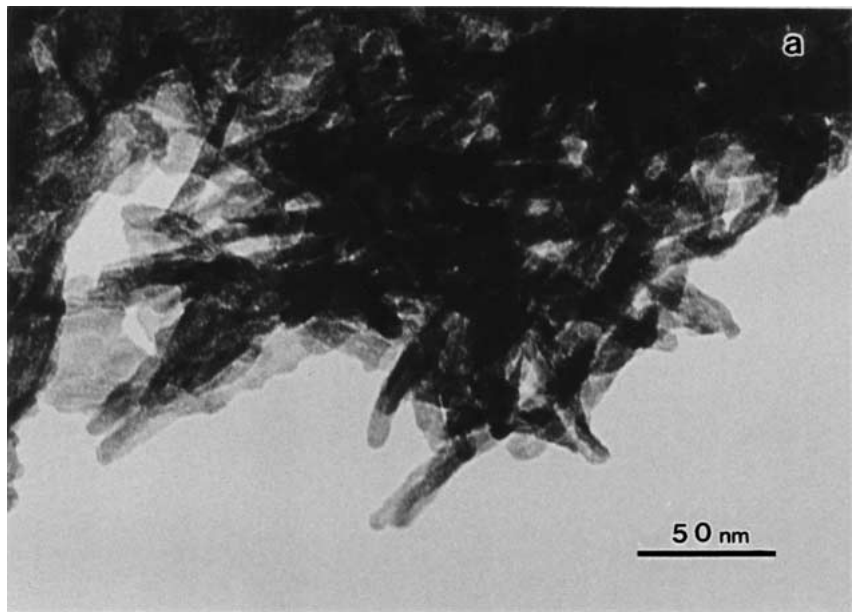

Figure 4 TEM images of (a) 20 mol% Ca^{2+} doped $Ce(OH)_3$ (before H_2O_2 oxidation in Methods A and B), (b) 20 mol% CaO doped CeO_2 oxidized at pH 7 (Method B) and (c) 20 mol% CaO doped CeO_2 oxidized at pH 11 (Method C). (*Continued.*)

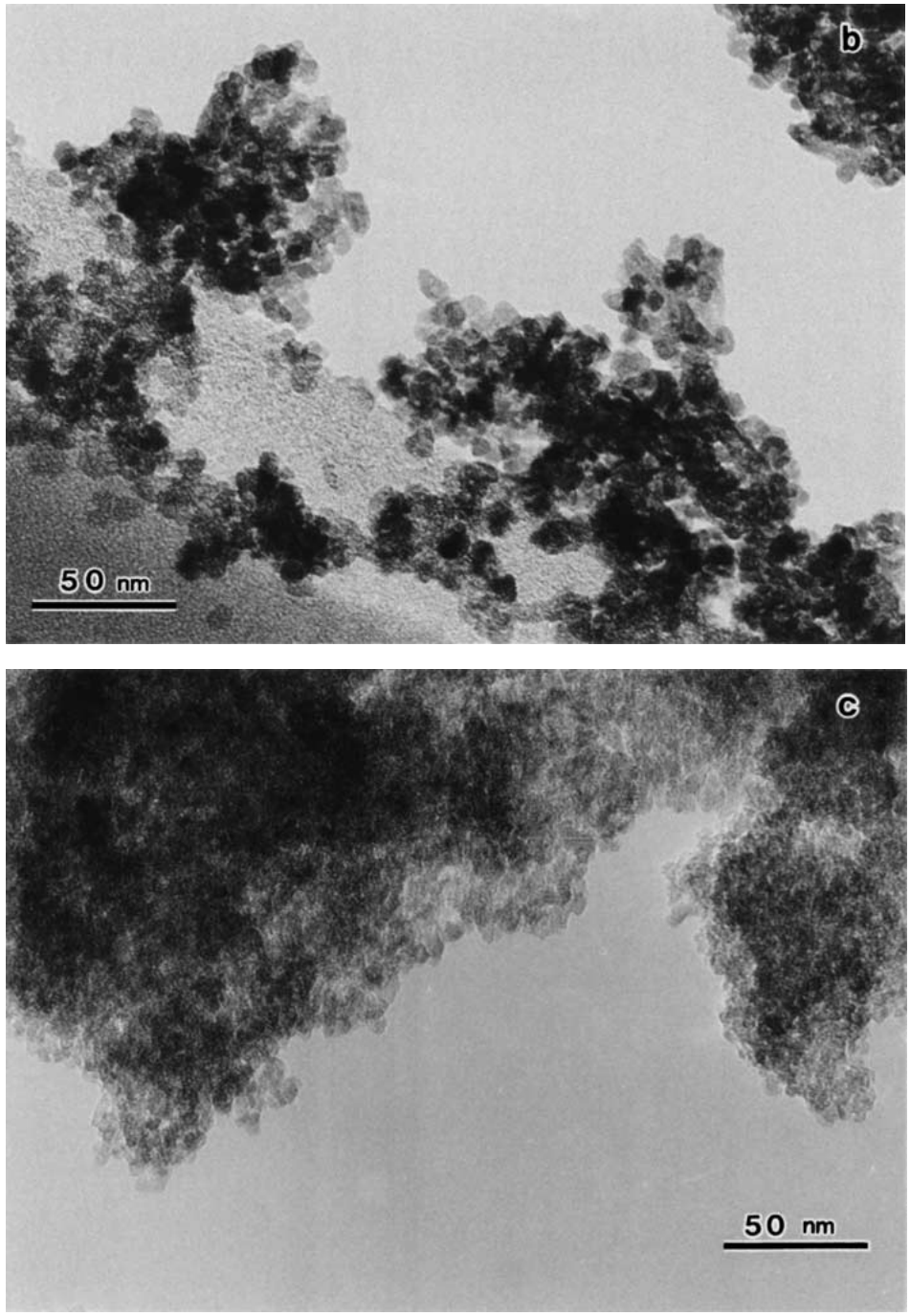

Figure 4 (*Continued.*)

during the oxidation reaction, we observed, with the TEM, that the rod-like $Ce(OH)_3$ particles had begun to separate into spherical shaped subunits after a few minutes to form spherical CeO_2. Therefore, the H_2O_2 oxidation reaction appeared to proceed by a topotactic reaction mechanism and a dissolution-precipitation mechanism in alkaline solution and acidic solution, respectively.

Furthermore, similar spherical particles of undoped and 20 mol% CaO doped CeO_2 were also obtained by conducting a neutralization reaction and oxidation reaction simultaneously by adding $CeCl_3$ and $CaCl_2$ mixed aqueous solution, NaOH aqueous solution and H_2O_2, simultaneously (method C). Fig. 4c shows the TEM image of the 20 mol% CaO doped CeO_2 adjusting the solution pH above 11 during the whole reactions. Although the pH of the solution was kept above 11, spherical nanoparticles of ceria were obtained. It may be due to the lack of time to grow rod-like $Ce(OH)_3$ particles since the nano sized spherical $Ce(OH)_3$ particles formed should be immediately oxidized to ceria under present reaction conditions. High resolution TEM image of Ca^{2+} doped $Ce(OH)_3$ are shown in Fig. 5. Large lod-like particles was not single crystal but consisted of small subunits ca. 5 nm in diameter. Matijevic [14, 15] has pointed out that the formation of spherical CeO_2 particles of narrow size distributions, consisting of a large number of small subunits, is caused by the uniformity of the latter and the chemical surface reactions taking place on their collisions. Similar reactions seemed to proceed in the formation of rod like $Ce(OH)_3$ particles under present reaction conditions. BET specific surface areas of undoped ceria, 20 mol% CaO doped ceria via method A and 20 mol% CaO

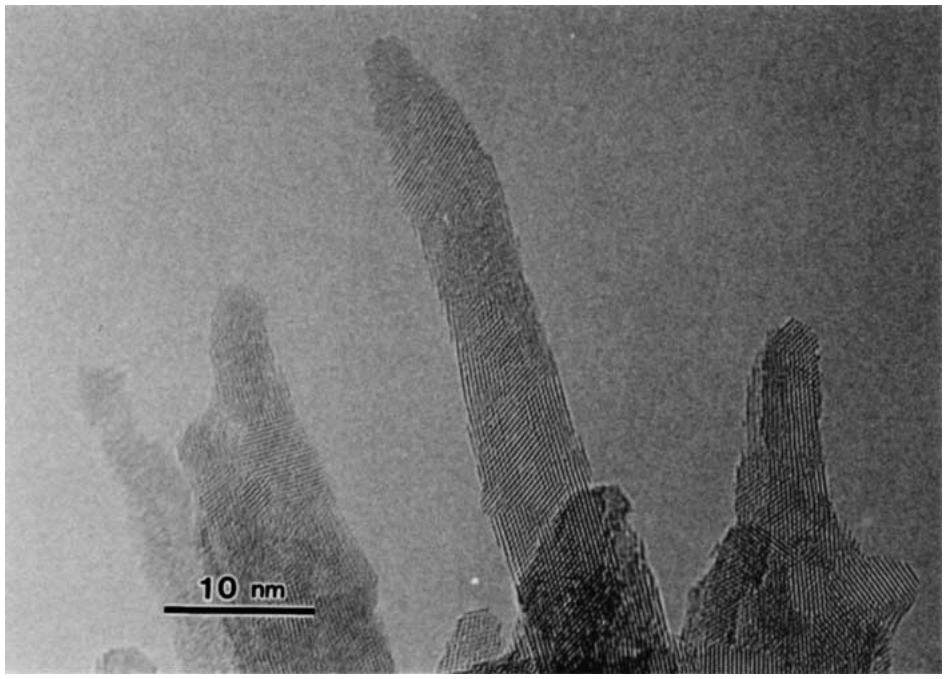

Figure 5 High resolution TEM images of 20 mol% Ca^{2+} doped $Ce(OH)_3$.

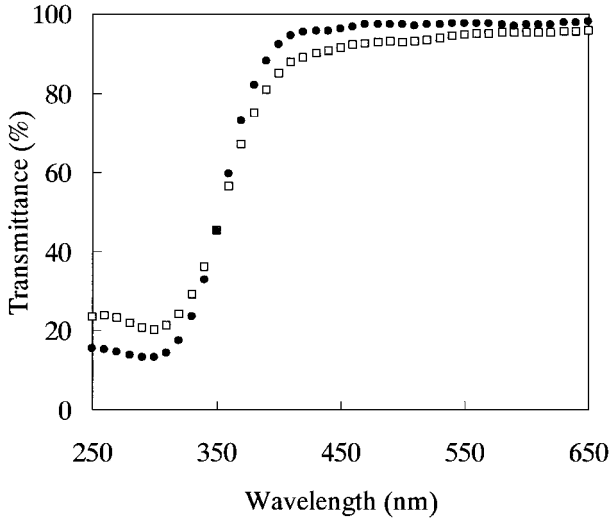

Figure 6 UV-Vis transmittance spectra of □ : undoped CeO_2 and ■ : 20 mol% CaO doped CeO_2 formed by Method A.

doped ceria via method C were 67, 111 and 101m^2/g, respectively.

UV-Vis transmittance spectra of (a) undoped CeO_2 and (b) 20 mol% CaO doped CeO_2 formed by Method A are shown in Fig. 6. CaO doped CeO_2 showed excellent UV-shielding capacity and high transparency in the visible light comparing with undoped CeO_2. The difference might be due to the difference in particle size. Namely, since the particle size of CaO doped CeO_2 was much smaller than that of undoped CeO_2, the particles dispersed well in the film and consequently could absorb UV-light more effectively. On the other hand, since the scattering of the light decreases with decreasing the particle size, the nanoparticles of CaO doped CeO_2 could show higher transparency in visible light region.

4. Conclusions

From the present results, following conclusions may be drawn. (1) Fine particles of calcia doped ceria, 2–4 nm in diameter, were prepared by the chemical reaction of $CeCl_3$-$CaCl_2$ mixed aqueous solution and NaOH aqueous solution at pH 6–12 and 40°C followed by the oxidation with hydrogen peroxide. (2) Doping CaO with CeO_2 resulted in decreasing the particle size and consequently, increasing UV shielding efficiency and transparency to visible light. (3) The particle shape of ceria changed significantly depending on the reaction condition, i.e., rod-like particles and spherical particles were formed by the H_2O_2 oxidation of cerium hydroxide above 8 and below 7, respectively.

References

1. F. IMOTO, T. NANATAKI and S. KANEKO, *Ceram. Trans.* **1** (1988) 204.
2. W. P. HSU, L. RÖNNIQIST and E. MATIJEVIC, *Langmuir* **4** (1988) 31.
3. P. L. CHEN, I. W. CHEN and S. KANEKO, *Am. Cerm. Soc.* **76** (1993) 1577.
4. Y. C. ZHOU and M. N. RAHAMAN, *J. Mater. Res.* **8** (1993) 1680.
5. A. TSCHÖPE and J. Y. YING, *Nanostruct. Master.* **4** (1994) 617.
6. Y. ZHOU, R. J. PHILLIPS and J. A. SWITZER, *J. Amer. Ceram. Soc.* **78** (1995) 981.
7. M. HIRANO and E. KATO, *ibid.* **79** (1996) 777.
8. W. CHEBGYUN, Q. YITAI, W. CHANGSUI, Y. LI and Z. GUIWEN, *Mater. Sci. Eng.* **B39** (1996) 160.
9. T. MASUI, K. FUJIKAWA, K. MACHIDA, T. SAKATA, H. MORI and G. ADACHI, *Chem. Mater.* **9** (1997) 2197.
10. T. MASUI, K. MACHIDA, T. SAKATA, H. MORI and G. ADACHI, *J. Alloys Compounds* (1997) 127.
11. X. YU, F. LI, X. YE, X. XIN and Z. XUE, *J. Amer. Ceram. Soc.* **83** (2000) 964.
12. S. YABE and S. MOMOSE, *J. Soc. Cosmet. Chem. Jpn.* **32** (1998) 372.
13. S. YABE, *Rare Earth* **35** (1999) 47.
14. E. MATIJEVIC, *Langmuir* **10** (1994) 8.
15. E. MATIJEVIC and W. P. HSU, *J. Colloid Interface Sci.* **118** (1987) 506.

Received 3 May
and accepted 2 October 2001